Available online at www.sciencedirect.com
SCIENCE DIRECT®
Nuclear Instruments and Methods in Physics Research A 535 (2004) 374–378
NUCLEAR INSTRUMENTS & METHODS IN PHYSICS RESEARCH Section A
www.elsevier.com/locate/nima

Test of CMS tracker silicon detector modules with the ARC system

A. Affolder[a,*], M. Axer[b], D. Barge[a], F. Beißel[b], C. Campagnari[a], G. Flügge[b], T. Franke[b,1], B. Hegner[b], Th. Hermanns[b], St. Kasselmann[b], J. Incandela[a], S. Levy[a,2], J. Mnich[b], A. Nowack[b], O. Pooth[b], B. Patterson[a], M. Pöttgens[b]

[a] *Physics Department, University of California, Santa Barbara, CA 93106-5239, USA*
[b] *III. Physikalisches Institut B, RWTH Aachen, Physikzentrum, D-52056 Aachen, Germany*

On Behalf of the CMS silicon Strip Tracker (ST) Collaboration
Available online 17 August 2004

Abstract

The CMS Silicon Strip Tracker will be equipped with 16000 silicon microstrip detector modules covering a surface of approximately 200 m^2. The APV Readout Controller system was developed at RWTH Aachen, III. Physikalisches Institut in order to perform full readout tests of hybrids and modules at each production step. From the experience derived from initial module production, an automated fault finding algorithm has been developed which uses the full correlations between different electrical tests. The results of a recent production of over 250 Tracker Outer Barrel and 25 Tracker End Cap modules at UCSB demonstrate that the testing protocols are sufficient to find all known faults and that electrical module components produced have a high quality. The results are typical of all CMS tracker assembly and bonding sites.

PACS: 06.60.Mr; 29.40.−n; 29.40.Gx; 29.40.Wk

Keywords: ARC; CMS; Fault finding; Module; Module production; Quality control; Tracker

1. Introduction

The CMS Silicon Strip Tracker (SST) will consist of about 16,000 detector modules assembled in four discrete subsystems: the tracker inner barrel (TIB), the tracker inner disks (TID), the tracker outer barrel (TOB), and the tracker end caps (TEC). Each module is made up of a carbon

*Corresponding author. Tel.: +1-805-893-3125; fax: +1-805-893-8597.
E-mail address: affolder@hep.ucsb.edu (A. Affolder).
[1]Also for Correspondence.
[2]Currently at University of Chicago, Chicago, IL, USA.

0168-9002/$ - see front matter © 2004 Elsevier B.V. All rights reserved.
doi:10.1016/j.nima.2004.07.155

fiber support structure, a front end hybrid circuit, and one or two silicon sensors (see Refs. [1,2] for a more detailed description of the CMS Silicon Strip Tracker).

2. The ARC system

Due to the large number of industrial companies and research institutes necessary to build such a large scale system, it is essential to have simple, reproducible assembly and testing procedures among the different test centers. The APV Read-out Controller System (ARC) [3,4] was developed at RWTH Aachen, III. Physikalisches Institut to be the universal, compact electrical testing system used at the hybrid manufactures, APV bonding centers, the module assembly (gantry) centers, and the module bonding centers. Since all sites use identical testing systems, the uniformity of the testing results is improved greatly.

The minimal ARC system, used for hybrid testing, consists of a Windows PC which acts as a control device of an ARC board which is connected to a hybrid via an ARC front end adapter (shown in Fig. 1). For module testing, the system is extended with an LED controller (LEP 16), which can induce charge in the sensors using diodes emitting infrared light, and a high voltage controller (DEPP), which supplies the required bias voltage of the sensors.

3. Electrical testing

Once a module is produced, the electrical testing is performed in three stages, each progressively searching for errors in more detail. First, an I–V measurement of the silicon sensors is made using the DEPP board. Gross failures, which can be caused by damages to the sensors or by micro-discharges, are indicated by an increase in the bias current relative to the sensor probing.

Next, the functionality of the integrated circuits on the front-end hybrid is checked. Each front-end hybrid houses chips for amplifying and buffering the data (APV) [5], multiplexing (MUX) [6], decoding the trigger and clock signal (PLL) [7],

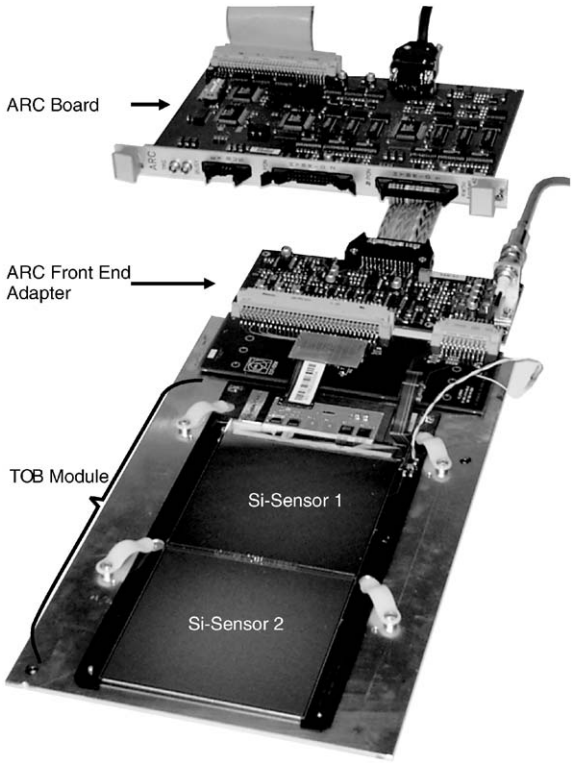

Fig. 1. Picture of a TOB module attached to a minimal ARC test system. The sensitive area consists of two wire bonded silicon strip sensors.

and monitoring the temperature and voltages of the module (DCU) [8]. For each chip, the I^2C based slow controls are tested, which are used for chip initialization, reading chip status, temperature, and voltage information. The response of each chip while varying initialization conditions are studied; at each stage, the power consumption of the chips are monitored to ensure proper chip functionality.

Finally, single channel faults are found using a set of tests. The faults could be in the APV, in the pitch adapter, in the sensors, or in the connections between them. The set of faults searched for are the following:

- *Opens*: breaks in the pitch adapter traces, missing wire bonds between the pitch adapter and a sensor or between two sensors, breaks in the aluminum strip in the sensors, and broken APV channels

- *Shorts*: connections between two channels in the pitch adapter, wire bonds, or sensors
- *Pinholes*: shorts between the aluminum strip and the p^+ implant of a channel in the sensor
- *Saturated channels*: channels in which the preamplifier of the APV is either dead or saturated and can no longer measure charge.

3.1. Fault identification algorithm

The type and location of the single channel faults are found using an algorithm which combines the three fault finding tests: a noise measurement, a charge injection using the APV's internal calibration circuit, and charge injection using an array of LEDs emitting infrared light.

Opens have lower load capacitances on the APV than good channels. As the noise of the channel increases linearly with the load capacitance, a *lower noise* is a good predictor of the presence and location of an open. The APV internal calibration circuit can be used to give a well defined amount of charge on an APV input. The shape of the signal stored in the APV depends on the load capacitance connected to the APV input. Smaller capacitances induce *faster rise times* and *higher pulse heights*. With these three test results, the location of an open can usually be determined.

Shorts can be easily discovered from the channels' response to the APV internal charge injection. Charge is injected into one channel at a time. In the presence of a short, the charge is shared between two channels, and therefore the pulse height will be typically *half as high* on two neighboring (or next-to-neighboring) channels. In addition, the noise of the channels will be irregular as twice the load capacitance is connected to each channel and the two channels' preamplifiers are also connected. Fig. 2 shows the calibration injection shape of various open and short types in a test module.

Finally, pinhole and saturated channels have similar noise and internal calibration responses. In both cases, the preamplifier of the APV can no longer measure charge; therefore, the noise will be low (non-zero due to the noise of the APV pipeline and readout) and the calibration injection pulse height will also be low.

Pinholes are differentiated from saturated channels using the LED system. For pinholes, the aluminum strip and thus the APV input is coupled resistively to the p^+ implant; therefore, the virtual

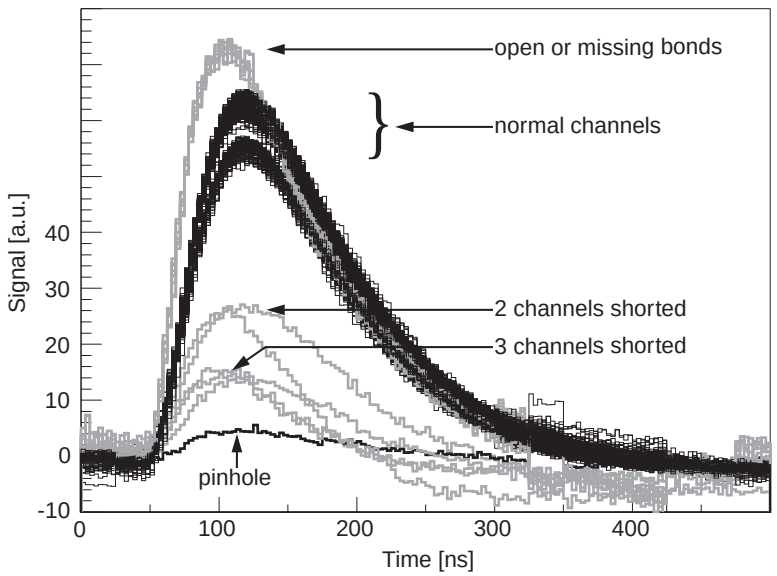

Fig. 2. Pulse shape of various fault types of a test module. Opens have a higher pulse height and a faster rise time. Shorts have approximately half the nominal pulse height. Pinholes or saturated channels show almost no response to charge injections.

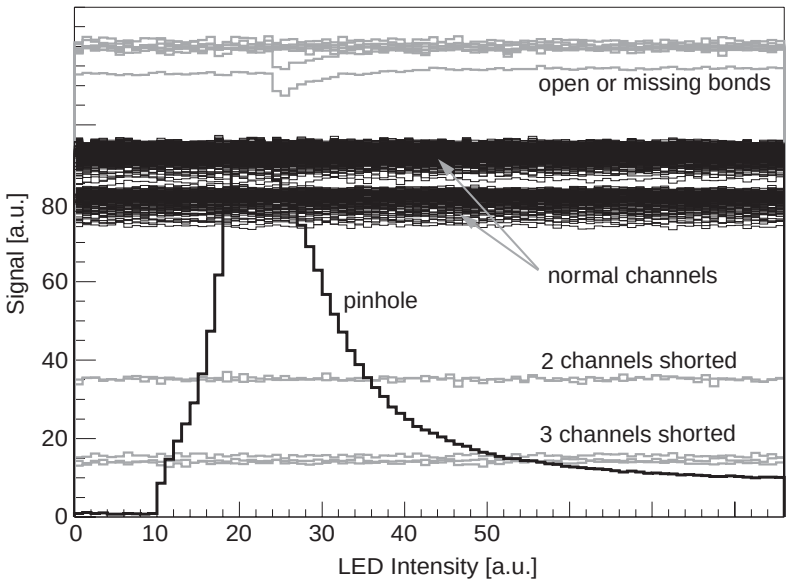

Fig. 3. The LED pinhole test result: the pinholed channel is initially saturated and has no calibration response. At a LED intensity of 25, the pinholed channel is unsaturated and the calibration pulse height matches a normal channel. Finally, at higher LED intensities, the channel becomes saturated again, and a lower calibration injection is seen.

ground of the APV will be at the voltage of the p^+ implant. The current flowing into/out of the APV depends on the resistance of the poly-silicon resistor, external resistors in the HV power return line and the leakage current through the bulk silicon. In the pinhole test, the LED is used to induce a higher leakage current in the bulk, which increases the voltage drop over the external resistors in the HV power return line and the poly-silicon resistors. With the proper leakage current, no current flows out of the APV and the channel becomes unsaturated. At this point, the channel will have a normal response to the internal calibration circuit. During the LED pinhole test, a bias current between 0 and 300 μA is induced using the LED array while the internal calibration circuit is pulsed. The pulse height is measured as a function of the LED intensity (bias current). Fig. 3 shows the result of the LED test of a module with a pinhole.

4. Test results at UCSB

A recent production of over 250 TOB modules and 25 TEC modules have been used to check/tune the fault finding algorithm. Similar studies have been performed or are underway by FNAL, the TIB collaboration in Italy, and the TEC collaboration in Central Europe. After the final tuning of the testing requirements, all known faults in the over 275 modules were found, leading us to believe that the fault finding algorithm is more than 99% efficient. The fault type and location was correctly identified in about 90% of the time. For those cases in which the fault type was not correctly determined, the different tests (noise vs. calibration injection) indicated different locations along the strip for open bonds (pitch adapter-to-sensor or sensor-to-sensor). In all cases, the correct location of the open bond was found by visual inspection. In addition, less than 0.1% of good channels are flagged as faulty. In most cases, these channels are the edge channels of the APVs that are known to have a special noise behaviour.

Prior to production, the goal was to produce modules with less than 2% faulty channels. As an indication of the high quality of the electrical modules components, the average rate

of the different fault sources of the modules are given:

- Hybrid wire bonding: 0.004%
- Module wire bonding: 0.003%
- Sensor faults: 0.39%.

On average, only 0.39% of the channels are found to be faulty, with less than 0.01% of the faults being introduced during the assembly and bonding process. These results are typical of modules containing two sensors produced for TOB and TEC. As TIB, TID, and inner TEC layers contain only one sensor, the fault rates for these detector subsystems are even lower.

5. Conclusions

The CMS Silicon Strip Tracker is currently under production. In order to test and characterize the approximately 16000 silicon microstrip detector modules needed, the APV Readout Controller (ARC) system was developed. Using the ARC system's custom HV power supply and LED system, a set of tests was established that efficiently finds and identifies the various possible faults in the modules. The algorithm developed finds more than 99% of the faulty channels with less than 0.1% good channels misidentified as faulty. In about 90% of all cases the error type is identified automatically.

Most misidentified faults are opens where the location of the missing bond is not predicted correctly. To demonstrate the extremely high electrical quality of the modules produced so far in the CMS Silicon Strip Tracker collaboration, the module production at UCSB is highlighted. During the production process, the rate of fault introduction is less than 0.1%; on average, the total fault rate is around 0.4%.

References

[1] The Tracker Project, Technical Design Report, CERN/LHCC 98-6 CMS TDR 5.
[2] CMS Collaboration, Addendum to the CMS Tracker TDR, CERN/LHCC 2000-016.
[3] M. Axer, et al., A test setup for quality assurance of frontend hybrids, CMS Note 2001/046.
[4] M. Axer, et al., Nucl. Instr. and Meth. A 518 (2004) 321.
[5] M.J. French, et al., Nucl. Instr. and Meth. A 466 (2001) 359.
[6] P. Murray, APVMUX User Guide, Version 1.0, 2000.
[7] P. Placidi, et al., CMS Tracker PLL Reference Manual, Version 2.1, 2000.
[8] G. Magazzu, et al., DCU2 User Guide, Version 2.12, 2001.